INSTITUT DE FRANCE
Académie des sciences

Comptes Rendus
Physique

Oliver Iff, Marcelo Davanco, Simon Betzold, Magdalena Moczała-Dusanowska, Matthias Wurdack, Monika Emmerling, Sven Höfling and Christian Schneider

Hyperspectral study of the coupling between trions in WSe_2 monolayers to a circular Bragg grating cavity

Volume 22, Special Issue S4 (2021), p. 97-105

Published online: 25 June 2021
Issue date: 8 March 2022

https://doi.org/10.5802/crphys.76

Part of Special Issue: Recent advances in 2D material physics

Guest editors: Xavier Marie (INSA Toulouse, Université Toulouse III Paul Sabatier, CNRS, France) and Johann Coraux (Institut Néel, Université Grenoble Alpes, CNRS, France)

e-ISSN : 1878-1535

Comptes Rendus
Physique
2021, 22, nº S4, p. 97-105
https://doi.org/10.5802/crphys.76

Recent advances in 2D material physics / *Physique des matériaux bidimensionnels*

Hyperspectral study of the coupling between trions in WSe_2 monolayers to a circular Bragg grating cavity

Oliver Iff[a], Marcelo Davanco[b], Simon Betzold[a], Magdalena Moczała-Dusanowska[a], Matthias Wurdack[c], Monika Emmerling[a], Sven Höfling[a,d] and Christian Schneider*[,e]

[a] Technische Physik and Wilhelm-Conrad-Röntgen Research Center for Complex Material Systems, Universität Würzburg, Am Hubland, Würzburg-97074, Germany

[b] Center for Nanoscale Science and Technology, NIST, Gaithersburg, 100 Bureau Drive, MD 20899, USA

[c] Nonlinear Physics Centre, Research School of Physics, The Australian National University, Canberra, ACT 2601, Australia

[d] SUPA, School of Physics and Astronomy, University of St. Andrews, St. Andrews KY16 9SS, UK

[e] Institute of Physics, University of Oldenburg, 26129 Oldenburg, Germany

E-mails: oliver.iff@physik.uni-wuerzburg.de (O. Iff), marcelo.davanco@nist.gov (M. Davanco), simon.betzold@uni-wuerzburg.de (S. Betzold), magdalena.moczala@uni-wuerzburg.de (M. Moczała-Dusanowska), Matthias.Wurdack@anu.edu.au (M. Wurdack), monika.emmerling@uni-wuerzburg.de (M. Emmerling), sven.hoefling@physik.uni-wuerzburg.de (S. Höfling), christian.schneider@uni-oldenburg.de (C. Schneider)

Abstract. Circular Bragg gratings compose a very appealing photonic platform and nanophotonic interface for the controlled light-matter coupling of emitters in nanomaterials. Here, we discuss the integration of exfoliated monolayers of WSe_2 with GaInP Bragg gratings. We apply hyperspectral imaging to our coupled system, and explore the spatio-spectral characteristics of our coupled monolayer-cavity system. Our work represents a valuable step towards the integration of atomically thin quantum emitters in semiconductor nanophotonic cavities.

Keywords. Circular Bragg grating, 2D materials, WSe_2, Quantum electrodynamics, Light matter coupling, Excitons.

Available online 25th June 2021

* Corresponding author.

1. Introduction

Atomically thin layers of transition metal dichalcogenides (TMDs) have advanced as a new material platform for on-chip optoelectronics, quantum photonics and to explore the limits of light-matter coupling [1–4]. In particular the giant dipole moment of excitons and coulomb-correlated multi-particle complexes in those materials makes them specifically appealing to explore the frontiers of cavity quantum electrodynamics. A variety of cavity quantum electrodynamics implementations with TMD layers were established and explored, including effects of weak [5–7], as well as strong coupling of excitons and photons [8–11]. To address challenges associated with capping TMD layers by dielectric or semiconductor layers [12], various strategies have been employed, such as open microcavity designs [13], flip-chip bonding [14, 15], and photonic crystal [16] or grating geometries featuring large electromagnetic field intensities at the surface [17]. While linear gratings have been shown to be valuable for achieving strong coupling in extended, one-dimensional configurations [17], circular gratings can also be harnessed to squeeze the optical mode into a very small volume. A circular Bragg grating (CBG), also referred to as a 'bullseye' cavity, has been successfully utilized in III–V quantum photonics to yield efficient single photon sources [18] and pair sources [19]. Recently, a first step towards the integration of atomically thin WSe_2 with a CBG has been discussed [20], where enhanced emission was observed from a monolayer. However, the experiments were conducted in the spectral range around 750 nm, where the emission of WSe_2 monolayers is usually dominated by a broad defect band at cryogenic temperatures, rather then the excitonic or trionic resonances located close to 720 nm [21]. Here, we investigate coupling of the WSe_2 trionic many-body resonance and close-by states near 720 nm to a CBG cavity, utilizing a hyperspectral imaging technique. We show evidence of selective coupling to one of the bullseye cavity's resonances by correlating emission spectra obtained from different locations across the geometry.

2. Sample characterization

Our CBG is based on an epitaxial heterostructure which was grown on a semi-insulating GaAs substrate and consists of a 1 μm thick $Al_{0.7}Ga_{0.3}As$ sacrificial layer, which is complemented by 120 nm of $Ga_{0.51}In_{0.49}P$ [22]. The fabrication of the CBG is sketched in Figure 1(a): first, the structure was spin-coated with polymethyl methacrylate (PMMA), and the CBG was defined by electron beam lithography and a short, subsequent reactive chemical etching step. Afterwards, the PMMA was removed, and larger holes were defined, surrounding the CBG. The process was completed by a selective wet chemical etch in hydrofluoric acid, to remove the sacrificial layer underneath the CBG. The scanning electron microscope images in Figures 1(b) and (c) depict the complete device, which is suspended, supported by the surrounding material.

In order to assess the optical modes supported by the CBG which may couple to TMD monolayer emitters, we utilized finite difference time domain (FDTD) calculations. The CBG features a well-defined optical mode that is concentrated at the center of the geometry (Figure 2(a)), and extends vertically, out of the sample plane, with a relatively small divergence angle (Figures 2(b) and (c)). Such mode allows spatially selective coupling to a TMD monolayer that is placed on the cavity, and efficient collection of the monolayer emitted light by free-space optics. As indicated in Figure 2(d), the cavity mode can furthermore be conveniently tuned through the emission spectrum of WSe_2 from below 700 nm and up to more than 800 nm by scaling the CBG inner disk and outer ring diameters with a factor ranging between 0.8 to 1.2. A maximum Purcell factor of up to 10 is preserved in all cases, as well as a relatively wide spectral bandwidth of approximately 10 nm.

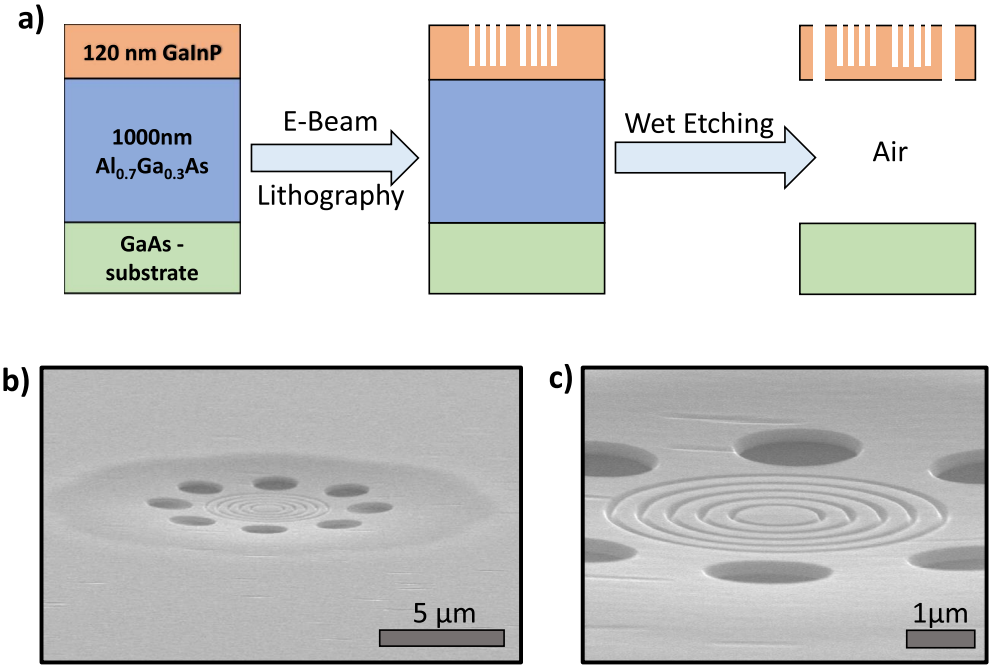

Figure 1. (a) Processing steps for a circular Bragg grating: onto a GaAs substrate a $Al_{0.7}Ga_{0.3}As$ sacrificial layer is grown, followed by a thin GaInP membrane. Via e-beam lithography the grating pattern is written into the membran and the sacrificial layer removed by wet etching through holes reaching it. (b) Scanning electron microscope (SEM) overview of the finished, under-etched membrane. (c) Close-up of the CBG.

3. Experiment and discussion

In order to study the coupling of TMD monolayer electronic resonances to the aforementioned photonic modes in our structure, we transferred a monolayer of WSe_2 onto a fabricated CBG, as shown in Figure 3(a) (see Methods for process details). After fabrication, a reflectivity spectrum was taken for the CBG, Figure 3(b), revealing a dip at approximately 730 nm consistent with the expected cavity mode spectral position. We next performed micron-scale, spatially-resolved micro-photoluminescence (PL) measurements of the fabricated structure. Importantly, since the monolayer spanned only an area of approximately 1 µm × 3 µm over the CBG, as seen in the scanning electron microscope (SEM) image of Figure 3(a), a spatially-resolved PL emission measurement was necessary to reveal a full picture of the light-matter coupling. Details of the measurement setup can be found in the Methods Section.

Figure 3(c) displays a spatially resolved PL map for emission at wavelength of 804 nm, solely capturing PL from the GaAs substrate that passes through the four larger circular holes that surround the CBG, similar to Figures 1(b) and (c). As such holes are placed symmetrically around the CBG, the GaAs emission can be used to determine the center position of the CBG (white crosses in Figures 3(c) and (d)). This was done by checking the alignment of the grating and the holes under an optical microscope. Based on that a crosshair was designed and visually matched to the GaAs emission peaks in the hyperspectral maps. Given a full-width at half-maximum of approximately 3 pixels for such peaks (approximately 1500 nm, for a pixel size of approximately 500 nm, see Methods), we estimate the center of the white cross to be well within

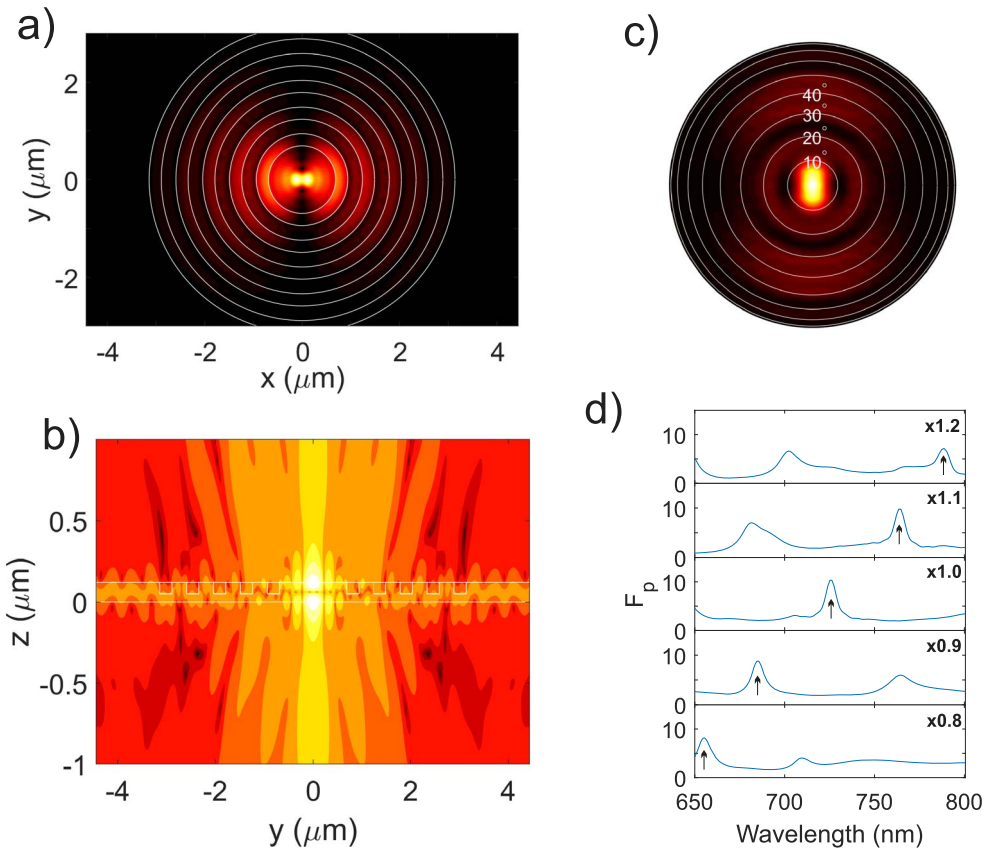

Figure 2. (a, b) Top and side view of the total electric field amplitude at 726 nm produced by a dipole placed right in the center and 10 nm above the GaInP membrane. The field is mainly confined in the inner disc and directed out-of-plane. A logarithmic color scale was chosen in (b) to facilitate visualization of the field inside and out of the semiconductor). (c) Finite difference time domain (FDTD) simulated far-field of a CBG showing a strong out-of-plane emission in the center region within a less than 0.17 rad (10°) angle. (d) Available mode tuning when scaling the CBG geometry dimensions by a factor of 0.8 to 1.2. The mode at around 730 nm for a scaling factor of 1.0 (arrow) exhibits a simulated Purcell-enhancement of up to 10.

the approximately 1600 nm diameter of the CBG's bullseye. Integrating the PL intensity between 700 nm and 780 nm, in contrast, we capture the emission intensity profile of the monolayer (see Figure 3(d)). Indeed, this profile is slightly shifted with respect to the center of the CBG, which suggests that only selected parts of the spectrum couple efficiently to the optical resonance supported by the cavity.

In Figure 4(a) spectra selected from specific locations over the CBG (indicated by circular dots on Figure 4(c)) are plotted, to compare the influence of the CBG on the emission properties. We observe that the CBG selectively enhances the luminescence around 730 nm, including the trionic resonance (X-) [21] and the peaks labeled as P0 and P1. The spectral region where the enhancement is observed falls within the reflectivity dip assigned to the CBG cavity mode.

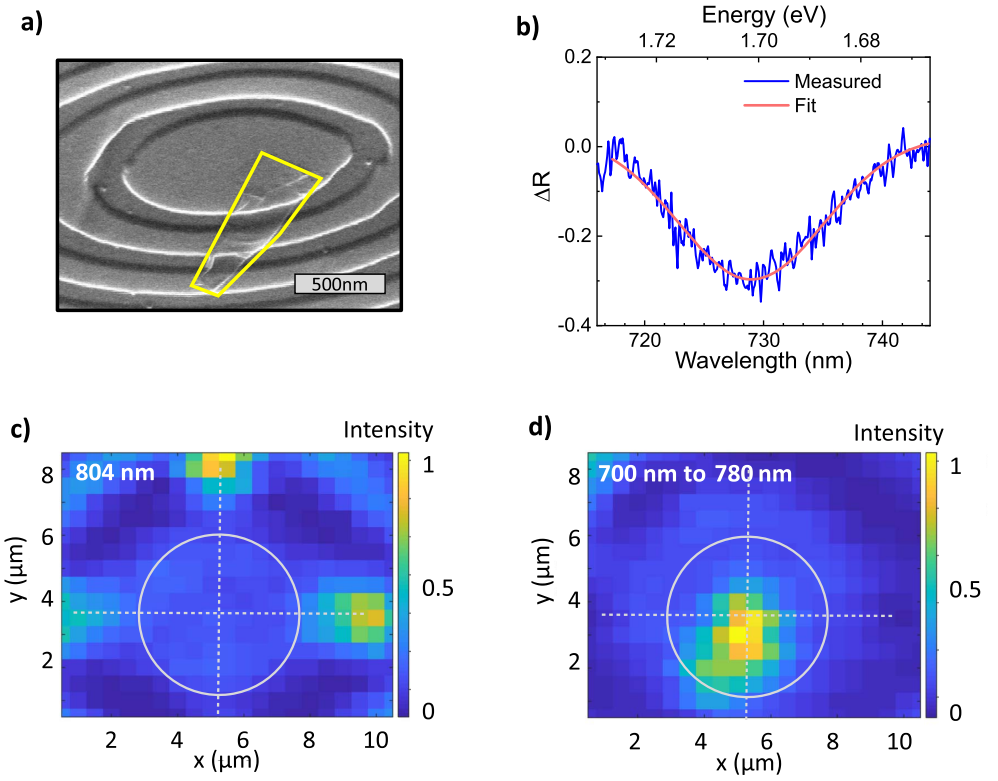

Figure 3. (a) SEM image of a WSe_2 monolayer (yellow) transferred onto a CBG. The image is rotated by 180° to align with the photoluminescence (PL) maps. (b) Reflectivity spectrum revealing the expected mode around 730 nm. Here, $\Delta R = R_{\mathrm{CBG}} - R_{\mathrm{ref}}$, where R_{CBG} and R_{ref} are respectively the reflectivities of the CBG and a reference silver mirror, normalized to their respective maxima within the displayed range. The red line is a fit with a Lorentzian line function. (c) PL map (pixel size: 0.5 μm × 0.5 μm) of the CBG at 804 nm revealing the GaAs emission that passes through the four etched holes around the grating. Based on this the position of the CBG is determined (white cross). The white circle represents the full extent of the CBG. (d) Integrated PL map between 700 nm to 780 nm owing to the monolayer emission.

The spectra outside of the CBG, where no monolayer is placed, is included as a baseline. Fitting both spectra on the monolayer (see Supplement S2 for details) reveals an increase of the intensity in the center compared to the edge of the CBG. The relative increasement is plotted in Figure 4(b), displaying a direct correlation of the enhancement on the overlap with the cavity mode. In contrast, the luminescence of P2 at 750 nm, which is assigned to defects in the WSe_2, remains mostly unaffected by the CBG. This spatio-spectral selective enhancement can be optimally visualized by comparing the integrated spatial luminescence pattern inside the mode in Figure 4(c) to outside of the mode (Figure 4(d)). Here, we indeed observe that the emission around 730 nm is most prominent in the center of the CBG, which indicates coupling to the CBG mode. In contrast, the luminescence features in the range between 740 nm and 780 nm solely reflect the location of the monolayer in the device, without any influence of the photonic mode structure.

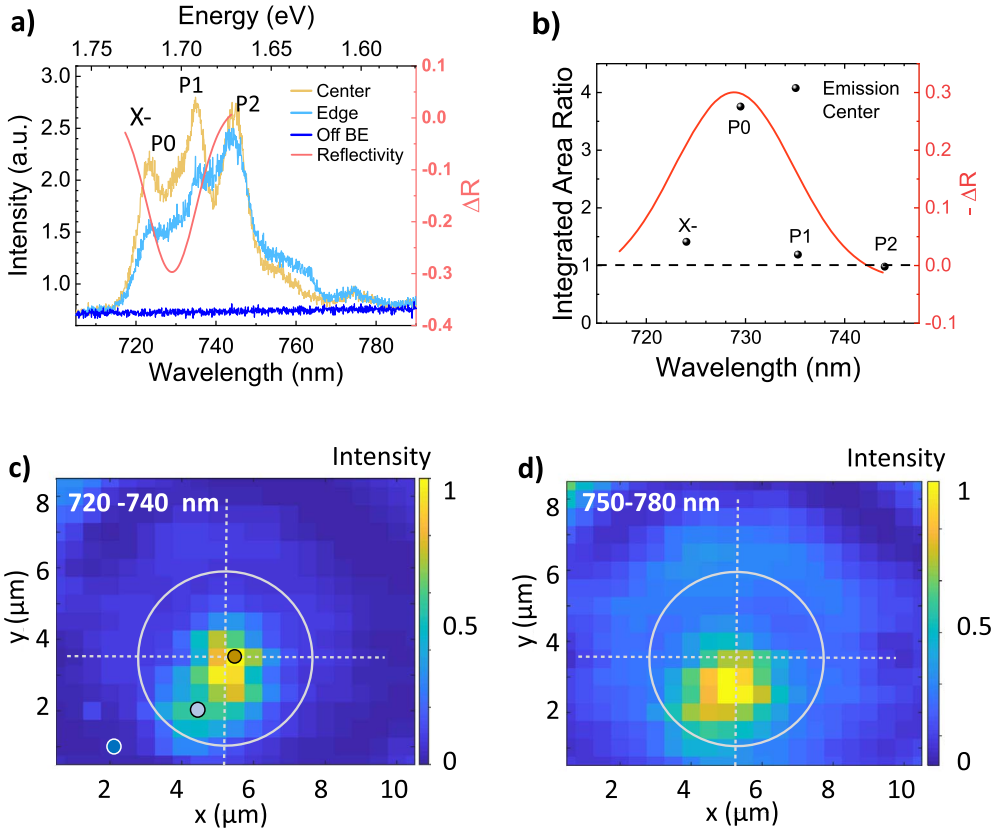

Figure 4. (a) Selected spectra at different positions on the CBG as shown in (c). X- marks the trion emission, P0, P1 and P2 additional signals typical found in WSe_2, respectively. (b) The ratio of the integrated area Center/Edge of the four labeled peaks in (a) show a correlation to the position of the cavity mode (displayed $-\Delta R$ for clarity). X-, P0 and P1 exhibit a enhancement of their intensity of up to 3.8. (c) Integrated photoluminescence in the range of 720 nm to 740 nm, covering the range of the mode and mainly positioned in the center of the CBG. (d) Integrated photoluminescence from 740 nm to 780 nm, which mainly follows the flake geometry. In (c) and (d), the white circle represents the full extent of the CBG, whereas dotted crosses indicate its center.

4. Summary

In conclusion, we have studied the light-matter coupling of a monolayer WSe_2 with the localized mode in a circular Bragg grating cavity via hyperspectral imaging. We clearly observe a spatial-sensitive enhancement of the emission of the monolayer. Importantly, the spatial profile of the weakly coupled photoluminescene follows the expected cavity resonance spatial profile, whereas the uncoupled broadband emission merely reflects the spatial shape of the mononolayer itself.

Our work is a first step towards highly scalable cavity quantum electrodynamics with engineered quantum emitters in two dimensional materials [23]. We envision, that full encapsulation of the TMD monolayer with a top and bottom hBN layer [24], combined with an optimized cleaning and annealing procedure, is a promising route to improve the coupling signatures in our system. At the conceptual stage, assembling such a Van-der-Waals heterostack on a CBG

should be straight forward, as the membranes are robust enough to withstand several transfer processes.

We further notice, that thus far, the community is still lacking solid evidence for the improved optical quality of WSe_2 single photon emitters arising from trapped excitons after full encapsulation with hBN, where even monolayers in the vicinity of metallic surfaces displayed very narrow spectral linewidths [25]. Hence, it could be appealing to test modified schemes utilizing metallic CBG structures [26] combined with atomically thin crystals, to significantly increase the available Purcell enhancement without deteriorating the optical quality of the emitters.

5. Methods

Sample fabrication. Monolayers of WSe_2 were mechanically exfoliated [27] via commercial adhesive tape from bulk WSe_2 crystals onto a PDMS stamp, and subsequently transferred onto the sample.

Optical spectroscopy. Spatially and spectrally resolved photoluminescence measurements, which were carried out on the sample attached to liquid helium flow cryostat at temperature of 5 K. We excited the sample with a 532 nm CW laser and collected the PL signal with an objective (50× and 0.42 NA). Collected PL light was diverted towards a grating spectrometer through a beamsplitter, and the reflected excitation laser was filtered by a long-pass color filter (630 nm). The signal was then analyzed by selecting a 1500 grooves/mm grating for higher resolution and 300 grooves/mm for capturing full spectrum, using a spectrometer consisting of a liquid nitrogen cooled charged coupled device. We estimate the illumination spot-size to be of approximately 2.5 μm in diameter, based on imaging with a CCD camera.

To obtain PL spatial maps, the cryostat was mounted onto two linear stages, which allowed the excitation and collection spot to be translated across the sample. The stages had a specified nominal resolution of 200 nm, and were scanned with a step-size of 500 nm to produce the hyperspectral images in Figures 3 and 4. We estimate the uncertainty in the coordinates for the collection spot in Figures 3 and 4 to be of approximately 400 nm, consistent with the nominal resolution of the stages, and smaller than the scan grid step.

Reflectivity spectrum. To obtain the cavity reflectivity spectrum of Figure 3(b), a similar illumination setup was used to illuminate the fabricated device with broadband light from a supercontinuum laser source. The reflected light stemming from the collection objective was, likewise to the PL collection case, diverted towards a grating spectrometer for spectral analysis. A reference reflectivity spectrum was obtained in a similar fashion from a silver mirror, normalized, and subtracted from the (normalized) CBG spectrum to produce the data plotted in Figure 3(b).

Acknowledgements

We thank Vasilij Baumann for supervising the growth of our samples and Kartik Srinivasan for the valueable discussions. We acknowledge the funding by the State of Bavaria and this work has been supported by European Research Council within the Project unLiMIt-2D (Project No. 679288).

Supplementary data

Supporting information for this article is available on the journal's website under https://doi.org/10.5802/crphys.76 or from the author.

References

[1] Q. H. Wang, K. Kalantar-Zadeh, A. Kis, J. N. Coleman, M. S. Strano, "Electronics and optoelectronics of two-dimensional transition metal dichalcogenides", *Nat. Nanotechnol.* **7** (2012), no. 11, p. 699-712.

[2] G. Wang, A. Chernikov, M. M. Glazov, T. F. Heinz, X. Marie, T. Amand, B. Urbaszek, "Colloquium: Excitons in atomically thin transition metal dichalcogenides", *Rev. Mod. Phys.* **90** (2018), no. 2, article no. 021001.

[3] K. F. Mak, J. Shan, "Photonics and optoelectronics of 2D semiconductor transition metal dichalcogenides", *Nat. Photonics* **10** (2016), no. 4, p. 216-226.

[4] J. S. Ponraj, Z.-Q. Xu, S. C. Dhanabalan, H. Mu, Y. Wang, J. Yuan, P. Li *et al.*, " Photonics and optoelectronics of two-dimensional materials beyond graphene", *Nanotechnology* **27** (2016), no. 46, article no. 462001.

[5] J. Kern, A. Trügler, I. Niehues, J. Ewering, R. Schmidt, R. Schneider, S. Najmaei, A. George *et al.*, "Nanoantenna-enhanced light-matter interaction in atomically thin WS_2", *ACS Photonics* **2** (2015), no. 9, p. 1260-1265.

[6] S. Butun, S. Tongay, K. Aydin, "Enhanced light emission from large-area monolayer MoS_2 using plasmonic nanodisc arrays", *Nano Lett.* **15** (2015), no. 4, p. 2700-2704.

[7] Y. J. Noori, Y. Cao, J. Roberts, C. Woodhead, R. Bernardo-Gavito, P. Tovee, R. J. Young, "Photonic crystals for enhanced light extraction from 2D materials", *ACS Photonics* **3** (2016), no. 12, p. 2515-2520.

[8] N. Lundt, A. Maryński, E. Cherotchenko, A. Pant, X. Fan, S. Tongay, G. Sek *et al.*, "Monolayered $MoSe_2$: A candidate for room temperature polaritonics", *2D Mater.* **4** (2016), no. 1, article no. 015006.

[9] X. Liu, T. Galfsky, Z. Sun, F. Xia, E. C. Lin, Y. H. Lee, S. Kéna-Cohen, V. M. Menon, "Strong light-matter coupling in two-dimensional atomic crystals", *Nat. Photonics* **9** (2014), no. 1, p. 30-34.

[10] Q. Wang, L. Sun, B. Zhang, C. Chen, X. Shen, W. Lu, "Direct observation of strong light-exciton coupling in thin WS_2 flakes", *Opt. Express* **24** (2016), no. 7, p. 7151-7157.

[11] C. Schneider, M. M. Glazov, T. Korn, S. Höfling, B. Urbaszek, "Two-dimensional semiconductors in the regime of strong light-matter coupling", *Nat. Commun.* **9** (2018), no. 1, article no. 2695.

[12] H. Knopf, N. Lundt, T. Bucher, S. Höfling, S. Tongay, T. Taniguchi, K. Watanabe, I. Staude *et al.*, "Integration of atomically thin layers of transition metal dichalcogenides into high-Q, monolithic Bragg-cavities: an experimental platform for the enhancement of the optical interaction in 2D-materials", *Opt. Mater. Express* **9** (2019), no. 2, p. 598-610.

[13] S. Schwarz, S. Dufferwiel, P. M. Walker, F. Withers, A. A. Trichet, M. Sich, F. Li *et al.*, "Two-dimensional metal-chalcogenide films in tunable optical microcavities", *Nano Lett.* **14** (2014), no. 12, p. 7003-7008.

[14] N. Lundt, Ł. Dusanowski, E. Sedov, P. Stepanov, M. M. Glazov, S. Klembt, M. Klaas, J. Beierlein *et al.*, "Optical valley Hall effect for highly valley-coherent exciton-polaritons in an atomically thin semiconductor", *Nat. Nanotechnol.* **14** (2019), no. 8, p. 770-775.

[15] C. Rupprecht, N. Lundt, M. Wurdack, P. Stepanov, E. Estrecho, M. Richard, E. A. Ostrovskaya *et al.*, "Micro-mechanical assembly and characterization of high-quality Fabry–Pérot microcavities for the integration of two-dimensional materials", *Appl. Phys. Lett.* **118** (2021), no. 10, article no. 103103.

[16] S. Wu, S. Buckley, A. M. Jones, J. S. Ross, N. J. Ghimire, J. Yan, D. G. Mandrus, W. Yao *et al.*, "Control of two-dimensional excitonic light emission via photonic crystal", *2D Mater.* **1** (2014), no. 1, article no. 011001.

[17] L. Zhang, R. Gogna, W. Burg, E. Tutuc, H. Deng, "Photonic-crystal exciton-polaritons in monolayer semiconductors", *Nat. Commun.* **9** (2018), no. 1, article no. 713.

[18] S. Ates, L. Sapienza, M. Davanco, A. Badolato, K. Srinivasan, "Bright single-photon emission from a quantum dot in a circular bragg grating microcavity", *IEEE J. Sel. Top. Quantum Electron.* **18** (2012), no. 6, p. 1711-1721.

[19] J. Liu, R. Su, Y. Wei, B. Yao, S. F. C. da Silva, Y. Yu, J. Iles-Smith, K. Srinivasan *et al.*, "A solid-state source of strongly entangled photon pairs with high brightness and indistinguishability", *Nat. Nanotechnol.* **14** (2019), no. 6, p. 586-593.

[20] N. M. H. Duong, Z. Q. Xu, M. Kianinia, R. Su, Z. Liu, S. Kim, C. Bradac, T. T. Tran *et al.*, "Enhanced emission from WSe_2 monolayers coupled to circular bragg gratings", *ACS Photonics* **5** (2018), no. 10, p. 3950-3955.

[21] A. M. Jones, H. Yu, N. J. Ghimire, S. Wu, G. Aivazian, J. S. Ross, B. Zhao, J. Yan *et al.*, "Optical generation of excitonic valley coherence in monolayer WSe_2", *Nat. Nanotechnol.* **8** (2013), no. 9, p. 634-638.

[22] O. Iff, Y.-M. He, N. Lundt, S. Stoll, V. Baumann, S. Höfling, C. Schneider, "Substrate engineering for high-quality emission of free and localized excitons from atomic monolayers in hybrid architectures", *Optica* **4** (2017), no. 6, p. 669-673.

[23] O. Iff, Q. Buchinger, M. Moczaa-Dusanowska, M. Kamp, S. Betzold, M. Davanco, K. Srinivasan, S. Tongay *et al.*, "Purcell-enhanced single photon source based on a deterministically placed WSe_2 monolayer quantum dot in a circular Bragg grating cavity", *Nano Lett.* (2021).

[24] F. Cadiz, E. Courtade, C. Robert, G. Wang, Y. Shen, H. Cai, T. Taniguchi, K. Watanabe, H. Carrere *et al.*, "Excitonic linewidth approaching the homogeneous limit in MoS_2-based van der Waals heterostructures", *Phys. Rev. X* **7** (2017), no. 2, p. 1-12.

[25] L. N. Tripathi, O. Iff, S. Betzold, M. Emmerling, K. Moon, Y. J. Lee, S.-H. Kwon, S. Höfling, C. Schneider, "Spontaneous

emission enhancement in strain-induced WSe_2 monolayer based quantum light sources on metallic surfaces", *ACS Photonics* **5** (2018), no. 5, p. 1919-1926.

[26] J. M. Yi, V. Smirnov, X. Piao, J. Hong, H. Kollmann, M. Silies, W. Wang, P. Grob *et al.*, "Suppression of radiative damping and enhancement of second harmonic generation in bull's eye nanoresonators", *ACS Nano* **10** (2016), no. 1, p. 475-483.

[27] A. Castellanos-Gomez, M. Buscema, R. Molenaar, V. Singh, L. Janssen, H. S. J. van der Zant, G. a. Steele, "Deterministic transfer of two-dimensional materials by all-dry viscoelastic stamping", *2D Mater.* **1** (2014), no. 1, article no. 011002.